

LINE-OF-SIGHT STATISTICAL METHODS FOR TURBULENT MEDIUM: VCS FOR EMISSION AND ABSORPTION LINES

D. Pogosyan, ¹ A. Lazarian ²

RESUMEN

ABSTRACT

We present an overview of the Velocity Coordinate Spectrum (VCS), a new technique for studying astrophysical turbulence that utilizes the line-of-sight statistics of Doppler-broadened spectral lines. We consider the retrieval of turbulence spectra from emission intensity observations of both high and low spatial resolution and find that the VCS allows one to study turbulence even when the emitting turbulent volume is not spatially resolved. This opens interesting prospects for using the technique for extragalactic research. VCS developed for spectral emission lines is applicable to absorption lines as well if the optical depth is used instead of intensity. VCS for absorption lines in point-source spectra benefit from effectively narrow beam and does not require dense sky coverage by sampling directions. Even strongly saturated absorption lines still carry the information about the small scale turbulence, albeit limited to the wings of a line. Combining different absorption lines one can develop tomography of the turbulence in the interstellar gas in all its complexity.

Key Words: TURBULENCE — ISM: GENERAL, STRUCTURE — MHD — RADIO LINES: ISM.

1. INTRODUCTION

Turbulence is a key element of the dynamics of astrophysical fluids, including those of interstellar medium (ISM), clusters of galaxies and circumstellar regions. The realization of the importance of turbulence induces sweeping changes, for instance, in the paradigm of ISM. It became clear, for instance, that turbulence affects substantially star formation, mixing of gas, transfer of heat. Observationally it is known that the ISM is turbulent on scales ranging from AUs to kpc (see Elmegreen & Scalo 2004), with an embedded magnetic field that influences almost all of its properties.

Using a statistical description is a nearly indispensable strategy when dealing with turbulence. One of the most widely used statistical measures is the turbulence spectrum, which describes the distribution of turbulent fluctuations over scales. For instance, the famous Kolmogorov model of incompressible turbulence predicts that the difference in velocities at different points in turbulent fluid increases on average with the separation between points as a cubic root of the separation, i.e. $|\delta v| \sim l^{1/3}$. In terms of direction-averaged energy spectrum this gives the famous Kolmogorov scaling $E(k) \sim 4\pi k^2 P(\mathbf{k}) \sim k^{5/3}$, where $P(\mathbf{k})$ is a 3D energy spectrum defined as the

Fourier transform of the correlation function of velocity fluctuations $\xi_v(\mathbf{r}) = \langle \delta v(\mathbf{x}) \delta v(\mathbf{x} + \mathbf{r}) \rangle$. Other types of turbulence, i.e. the turbulence of non-linear waves or the turbulence of shocks, are characterized by different power laws and therefore can be distinguished from the Kolmogorov turbulence of incompressible eddies. Substantial advances in our understanding of the scaling of compressible MHD turbulence (see review by Cho & Lazarian 2005, and references therein) allows us to provide a direct comparison of theoretical expectations with observations.

Recovering the velocity spectra from observations is a challenging problem. Observations provide integrals of either emissivities or opacities, both proportional to the local densities, in Position-Position Velocity space (henceforth PPV), i.e as a function of the direction on the sky and frequency that can be viewed as the position in velocity coordinate along the line of sight. Statistical measurements in this space are affected both by inhomogeneous spatial distribution and the motion of the matter. Turbulence is associated with fluctuating velocities that cause fluctuations in the Doppler shifts of emission and absorption lines. If turbulence is supersonic, the recovering of its velocity spectrum is possible with the Velocity Channel Analysis (VCA) of the emission intensity maps (Lazarian & Pogosyan 2000, 2004, LP00,LP04). This technique has been successfully applied in several papers starting with Stanimirović & Lazarian (2001). However, the VCA

¹University of Alberta, Edmonton, Canada, pogosyan@ualberta.ca

²University of Wisconsin, Madison, USA, lazarian@astro.wisc.edu

arXiv:0902.0011v1 [astro-ph.GA] 30 Jan 2009

is just one way to use the general description of fluctuations in the PPV space. One can also study fluctuations along the *velocity coordinate*. The corresponding technique was termed the Velocity Coordinate Spectrum in Lazarian (2004) and has been developed in Lazarian & Pogosyan (2006, LP06) for emission and in Lazarian & Pogosyan (2008, LP08) for absorption lines. In this presentation we give an overview of these developments.

2. LINKING OBSERVATIONAL AND TURBULENT STATISTICAL MEASURES

Let us consider a volume of turbulent gas or plasma (a “cloud”) which extent along the line of sight S is much smaller than the distance to the observer. Along a line of sight that is labeled by a two-dimensional position vector \mathbf{X} on the cloud image, the intensity in a spectral (either emission or absorption) line with rest-frame frequency ν_0 , $I_{\mathbf{X}}(\nu, \nu_0)$, is determined by the density of emitting (or absorbing) atoms in PPV space (LP06,LP08), $\rho_s(\mathbf{X}, v)$

$$I_{\mathbf{X}}(v) = \frac{\epsilon}{\alpha} \left[1 - e^{-\alpha \rho_s(\mathbf{X}, v)} \right] \quad \text{emission} \quad (1)$$

$$I_{\mathbf{X}}(v) = I_0 e^{-\alpha \rho_s(\mathbf{X}, v)} \quad \text{absorption} \quad (2)$$

where ϵ is the emissivity and α is the absorption³ coefficient. and the velocity $v \approx \frac{c}{\nu_0}(\nu - \nu_0)$, if the intrinsic line width is neglected.

In the simplest case of optically thin emission lines and unsaturated absorption lines the PPV density is directly connected to observables, the emission intensity or the optical depth for absorption

$$\rho_s(\mathbf{X}, v) \propto I_{\mathbf{X}}(v), \quad \alpha \rightarrow 0, \quad \text{emission} \quad (3)$$

$$\rho_s(\mathbf{X}, v) \propto \tau_{\mathbf{X}}(v) \equiv -\ln(I/I_0), \quad \text{absorption} \quad (4)$$

PPV density $\rho_s(\mathbf{X}, v)$ encodes the information about both the turbulent velocities and the inhomogeneity in the matter distribution. The characteristic feature that allows us to distinguish between the thermal and turbulent velocity is the spatially correlated nature of the latter. Under set of assumptions employed in LP00 and LP04, the PPV structure function $d_s(R, v) = \langle [\rho_s(\mathbf{X}_1, v_1) - \rho_s(\mathbf{X}_2, v_2)]^2 \rangle$, $R = |\mathbf{X}_1 - \mathbf{X}_2|$, $v = |v_1 - v_2|$, can be expressed via real space velocity and density correlations as

$$d_s(R, v) \propto \int_{-S}^S dz \frac{\xi(r)}{\sqrt{D_z(\mathbf{r}) + 2\beta}} \exp \left[-\frac{v^2}{2(D_z(\mathbf{r}) + 2\beta)} \right], \quad (5)$$

³Self-absorption in case of emission line

where the structure function of the velocity z -components is

$$D_z(\mathbf{r}) \approx C r^m, \quad (6)$$

(C is a normalization constant) and for the density correlation function $\xi(\mathbf{r} = |\mathbf{x}_1 - \mathbf{x}_2|) = \langle \rho(\mathbf{x}_1) \rho(\mathbf{x}_2) \rangle$ the isotropic power-law form is adopted

$$\xi(r) \propto \left(1 + \left[\frac{r_0}{r} \right]^\gamma \right). \quad (7)$$

The thermal broadening is described by $\beta = \frac{k_B T}{m_a}$.

The Eq. (5) provides way for recovery of the turbulence by measuring the correlations of the observed signal, for example the structure functions

$$\left. \begin{aligned} \mathcal{D}(R, v) &\equiv \langle [I_{\mathbf{X}_1}(v_1) - I_{\mathbf{X}_2}(v_2)]^2 \rangle \\ \mathcal{D}(R, v) &\equiv \langle [\tau_{\mathbf{X}_1}(v_1) - \tau_{\mathbf{X}_2}(v_2)]^2 \rangle \end{aligned} \right\} \propto d_s(R, v) \quad (8)$$

Despite formal similarity, use of emission and absorption lines has also several distinct features.

Measuring the emission by the turbulent gas typically provides us with a sky map of the signal. If the angular resolution of such map is high, it is more advantageous to measure angular correlations across the image $\mathcal{D}(R, 0)$. This leads to the VCA analysis (LP00, LP04) that has been reviewed at the “Magnetic Fields in the Universe I” meeting (Pogosyan & Lazarian 2005). The use of the line-of-sight measure $\mathcal{D}(0, v)$ that we review here is more challenging but has an advantage for the data with poor angular resolution.

Absorption spectra, on the other hand, typically represents real pencil beams for which the line-of-sight statistics is the only one available. The effective angular resolution of such spectra is high if the source is a point object. Therefore both high and low angular resolution limits of the VCS are of interest. One can also applying VCS to the wings of saturated absorption lines (LP08) although the issues of noise, velocity resolution and intrinsic line broadening become critical for such studies.

3. VCS FOR A TRANSPARENT EMITTING MEDIUM

The intensity in optically thin lines provides direct information on the density in PPV space according to Eq. (8). Finite angular resolution of the instrument leads to the beam-averaged measurements

$$\mathcal{D}(0, v) = \int d\mathbf{R} B(\mathbf{R}) d_s(R, v). \quad (9)$$

where the realistic beam has a finite width, ΔB .

We shall formulate VCS results using the velocity coordinate power spectrum

$$P(k_v) = \int dv \mathcal{D}(0, v) \exp[-k_v^2 v^2 / 2] \quad (10)$$

where k_v is the “wave-number” reciprocal to the velocity v coordinate. With regard to the observation scale k_v , two other scales define the different regimes of the analysis:

From instrumental perspective it is resolution scale is important. To the linear scale ΔB corresponds the velocity scale

$$V_{\Delta B} \equiv \sqrt{D_z(S)(\Delta B/S)^m} \quad , \quad (11)$$

equal to the magnitude of turbulent velocities at the separation of a size ΔB . For a measurements at the scale k_v the beam is effectively narrow when

$$k_v < V_{\Delta B}^{-1} \quad (12)$$

while on shorter scales its width is important. Note that it is angular resolution that affects the behaviour of line-of-sight statistics. Similarly, for 2D VCA analysis in channel maps velocity resolution played a role in interpreting 2D statistics of intensity maps

From the perspective of the turbulence properties the amplitude of the density contribution to VCS is encoded in the correlation length r_0 . This scale decides whether density inhomogeneities dominate in Eq. (7) or the turbulence effects are manifest only in random motions of the uniform gas distribution, $\xi(r) = 1$. The velocity scale that corresponds to r_0 is

$$V_{r_0} = \sqrt{D_z(S)(r_0/S)^m} \quad , \quad (13)$$

So we can roughly equate the scale of equality of the density and velocity effects to r_0 , i.e., in velocity units,

$$k_v \approx V_{r_0}^{-1} \quad . \quad (14)$$

In Figure 1 we summarize the different scalings of VCS. As for the VCA the main difference stems from the density being either shallow or steep. If the density is shallow i.e. scales as $\xi \sim r^{-\gamma}$, $\gamma > 0$, which means that the correlations increase with the decrease of the scale, then it eventually becomes important at sufficiently small velocity differences, i.e. at sufficiently large k_v . In the opposite case, i.e. when $\gamma < 0$, the contributions of density can be important only at large velocity separations.

The left and middle panels of Figure 1 deal with the case of shallow density. Velocity is dominant at $k_v < k_0$, while the density term provides the main

contribution at $k_v > k_0$. The left panel demonstrates the case where the scale of transition from asymptotic is entirely dominated by velocity to the one influenced by spatially resolved velocity and density, $V_{\Delta B} < V_{r_0}$. The observed fluctuations arising from the unresolved turbulent eddies depends on the scalings of both velocity and density. In the middle panel, $V_{\Delta B} > V_{r_0}$, the transition scale is unresolved. In this case if there is still a dynamical range for moderately long scales to be resolved by the experiment $D_z(S)^{1/2} > k_v^{-1} > V_{\Delta B}$, the VCS of the resolved eddies will be determined by the turbulent velocities only.

The right panel of Figure 1 addresses the case of a steep density spectrum. The difference now is that fluctuations of the density are maximal at low wave-numbers and it is there that the density could be important. Velocity is dominant at shorter scales $k_v > k_0$. However, the steep density correlation length r_0 is large, at least as large as the density power cutoff r_c , which argues for density fluctuations to be subdominant everywhere up to the scale of the emitting turbulent volume (“cloud”).

3.1. Thermal effects and inertial range

In Figure 1 we have plotted theoretical power spectra over 3 decades of velocity magnitude to compactly demonstrate all possible scalings. Thermal effects are shown as well, which in a language of the power spectrum are simply described by $\exp[-\beta k_v^2]$ cutoff factor.

In observations, one can anticipate a coverage over two decades of velocity magnitudes before thermal effects get important. Potentially, correcting for the thermal broadening, one can extend the observational range further. Note, that the thermal corrections are different for species of different mass. Therefore, by using heavier species one can extend the high k cut-off by the square root of the ratio of the mass of the species to the mass of hydrogen.

How deeply subsonic scales can still be probed in cold gas depends on the signal-to-noise ratio of the available data. Indeed, the ability to deconvolve the thermal smoothing is limited by noise amplification in the process. However, any extension of the VCS by a factor a in velocity results in the extension of the sampled spatial scales by a factor of $a^{2/m}$, which is a^3 for the Kolmogorov turbulence.

Even with a limited k_v coverage, important results can be obtained with VCS, especially if observations encompass one of the transitional regimes. For example, if one measures a transition from a shallow spectrum to a steeper one (see the left and the

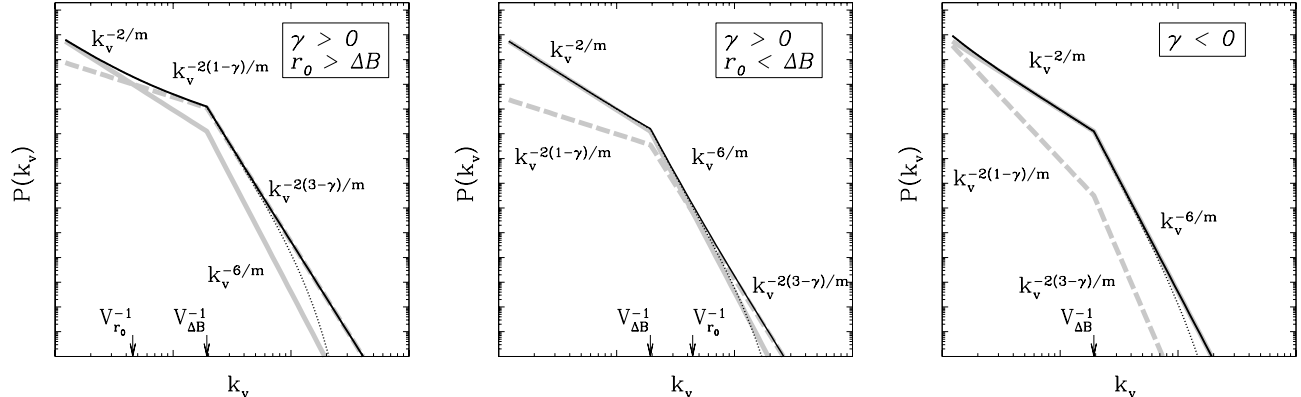


Fig. 1. Qualitative representation of the density and velocity contributions to the VCS power spectrum and the resulting scaling regimes. In every panel light lines show contributions from the ρ -term (density modified by velocity, dashed line) and v -term (pure velocity effect, solid line) separately, while the dark solid line shows the combined total VCS power spectrum. Thermal suppression of fluctuations is shown by the dotted line. The labels above the dark solid curve are arranged so as to illustrate the sequential transition of the scalings of the total power spectrum. Everywhere except the intermediate regimes, the total spectrum is dominated by one of the components to which the current labeled scaling corresponds. Labels below the dark solid lines mark the scaling of the subdominant contributions. For the left and middle panels the density power spectrum is taken to be shallow, $\gamma > 0$. The left panel corresponds to high amplitude of the density correlations, $r_0 > \Delta B$, where density effects become dominant at relatively long wavelengths for which the beam is narrow. In the middle panel, the amplitude of density correlations is low $r_0 < \Delta B$ and they dominate only the smallest scales which results in the intermediate steepening of the VCS scaling. The right panel corresponds to the steep density spectrum. In this case the density contribution is always subdominant. In this example the thermal scale is five times shorter than the resolution scale $V_{\Delta B}$.

right panels in Figure 1) one has the potential to i) determine the velocity index m , since the difference between the slopes is always $4/m$; ii) determine γ next; iii) estimate the amplitude of turbulent velocities from the position of the transition point as discussed above. On the other hand, if one encounters a transition from a steep to a shallower spectrum, one i) may argue for the presence of the shallow density inhomogeneities; ii) estimate γ/m from the difference of the slopes, and then m ; iii) estimate the density correlation radius r_0 . Finally, if no transition regime is available, then for $\gamma < 0$ one can get m , while for the case of $\gamma > 0$ a combination of γ and m is available.

4. VCS FOR ABSORPTION LINES

Studies of turbulence with absorption lines are possible with the VCS technique if, instead of intensity $I(\nu)$, one uses the optical depth $\tau(\nu)$, i.e., the logarithm of the absorbed intensity $\log I_{abs}(\nu)$.

In the weak absorption regime, i.e. when the optical depth at the middle of the absorption line is less than unity, the analysis of the $\tau(\nu)$ coincides with the analysis of emission discussed above, taken in the limit of ideal angular resolution.

In Figure 2 we summarize different regimes for studying turbulence using absorption lines from

point sources for which angular resolution can be considered as perfect. For shallow density, i.e. for $\xi(r) \approx \bar{n}^2 [1 + (r_0/r)^\gamma]$, $\gamma > 0$ the spectrum of optical depth fluctuations that arise from inhomogeneities in density projected onto velocity coordinate scales as $P_\rho(k_v) \sim k_v^{-2(3-\gamma)/m}$. For sufficiently large k_v its contribution dominates the contribution $P_v(k_v) \sim k_v^{-2/m}$ coming from purely velocity projection effect of turbulently moving uniformly distributed, $\xi(z) \approx \bar{n}^2$, gas. If we measure the point $\Delta V_{r_0} \approx \sqrt{D_z(S)}(r_0/S)^{m/2}$ at which P_ρ becomes dominant over P_v , we can estimate the density correlation radius r_0 which has the physical meaning of the scale at which the dispersion of the fluctuations of density equal the mean density (see LP06). However, whether we can observe both regimes or just one, depends on the mask that is imposed by the saturation of the absorption line, as well as the small scale filtering arising from thermal broadening. For $\gamma < 0$, P_v always dominates.

In the intermediate absorption regime, i.e. when the optical depth at the middle of the absorption line is larger than unity, but less than 10^3 , the wings of the absorption line can be used for the analysis. The central, saturated part of the line is expected to be noise dominated.

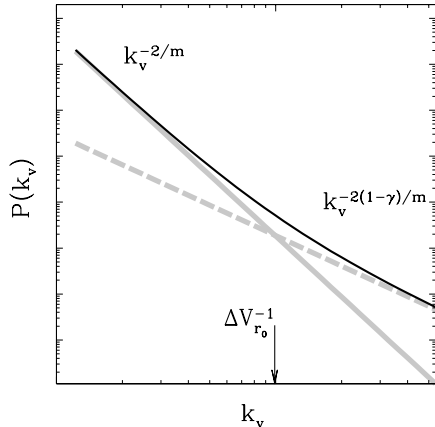


Fig. 2. Power spectrum of the optical depth fluctuations due to turbulent motions of absorbers in unsaturated absorption line. Thermal and intrinsic line smoothing is factored out. Effect of density inhomogeneities becomes dominant at $k_v > V_{r_0}^{-1}$, assuming shallow density, $\gamma > 0$.

Higher the absorption, less the extend of the wings available for the analysis is. In terms of the mathematical setting this introduces an additional window in the expressions for the VCS analysis. However, the contrast of the small scale fluctuations increases with the decrease of the window.

For strong absorption regime, the broadening is determined by Lorentzian wings of the line and therefore no information on turbulence is available.

5. VCS COOKBOOK

The VCS cookbook for emission lines is rather straightforward. VCS near a scale k_v depends on whether the instrument resolves the correspondent spatial scale $[k_v^2 D_z(S)]^{-1/m} S$, where S is the scale where turbulence saturates. If this scale is resolved then $P_v(k_v) \propto k_v^{-2/m}$ and $P_\rho(k_v) \propto k_v^{-2(1-\gamma)/m}$. If the scale is not resolved then $P_v(k_v) \propto k_v^{-6/m}$ and $P_\rho(k_v) \propto k_v^{-2(3-\gamma)/m}$. These results are presented in a compact form in Table 1. The transition from the low to the high resolution regimes happens as the velocity scale under study gets comparable to the turbulent velocity at the minimal spatially resolved scale. As the change of slope is the velocity-induced effect, it is not surprising that the difference in spectral indexes in the low and high resolution limit is $4/m$ for both P_v and P_ρ terms, i.e it does not depend on the density. This allows for separation of the velocity and density contributions. For instance, Figure 1 illustrates that in the case of shallow density both the density and velocity spectra can be obtained.

Note that obtaining the density spectrum from

a well resolved map of intensities is trivial for the optically thin medium, as the density spectrum is directly available from the column densities (i.e. velocity integrated intensities). However, for the absorbing medium such velocity-integrated maps provide the universal spectrum K^{-3} , where K is the 2D wavenumber (LP04). Similarly, even for the optically thin medium, it is not possible to get the density spectrum if the turbulent volume is not spatially resolved. On the contrary, $P_\rho(k_v)$ reflects the contribution of shallow density even in this case.

An advantage characteristic to absorption lines is that they provide measurements in the "high resolution regime", provided that the absorption against a point source is used. This is important, in particular, for turbulence research in extragalactic setting where even high angular resolution may not translate into high spatial resolution. To get proper statistical averaging, one requires more than one point source. Numerical experiments in Chepurnov & Lazarian (2006, 2008) showed that using measuring spectra along 5-10 lines of sight is enough to recover the underlying spectrum properly.

In the simplest case, Figure 2 illustrates how the information on velocity and density can be obtained from observations for the case of shallow density. In the case of steep density the measured spectrum is always $\sim k_v^{-2/m}$, which allows finding the spectral index of velocity m .

Similar to the case of emitting gas, the VCS study of absorbing gas is dominated by the coldest gas component. A practical emission data handling using the VCS technique in Chepurnov et al. (2006) showed that fitting the observed power spectrum using the integral expressions is a more reliable way of obtaining both parameters of the underlying turbulence and temperature of the emitting gas.

The difference in data analysis for absorption lines compared to that of Chepurnov et al. (2006) is twofold. Firstly, one has to take into account masking of the data that restricts it to the wings region if the line is saturated. Secondly, for emission maps analyzed in Chepurnov et al. (2006) the fitting was done while varying the spatial resolution of the data. As the effects of particular factors, e.g. thermal broadening, are different at different spatial scales, one can provide additional testing of the accuracy of the fit by varying the angular resolution. Varying the resolution is not an option for the absorption data from point sources but is possible when spatially extended sources are used to sample the medium. In the latter case the VCA-type studies of the absorption lines wings may also be possible.

TABLE 1

SCALINGS OF VCS $P(K_V) = P_\rho(k_v) + P_V(k_v)$ FOR SHALLOW AND STEEP DENSITIES.

Spectral term	$\Delta B < S [k_v^2 D_z(S)]^{-\frac{1}{m}}$	$\Delta B > S [k_v^2 D_z(S)]^{-\frac{1}{m}}$
$P_\rho(k_v)$	$\propto \left(k_v D_z^{1/2}(S)\right)^{-2(1-\gamma)/m}$	$\propto \left(k_v D_z^{1/2}(S)\right)^{-2(3-\gamma)/m}$
$P_V(k_v)$	$\propto \left(k_v D_z^{1/2}(S)\right)^{-2/m}$	$\propto \left(k_v D_z^{1/2}(S)\right)^{-6/m}$

REFERENCES

- Elmegreen, B. G., & Scalo, J. 2004, *ARA&A*, 42, 211
 Chepurnov, A., Lazarian, A., Stanimirovic, S., Peek, J. E. G., & Heiles, C. 2006, arXiv:astro-ph/0611462
 Chepurnov, A., & Lazarian, A. 2006, arXiv:astro-ph/0611465
 Chepurnov, A., & Lazarian, A. 2008, arXiv:0811.0845
 Cho, J., & Lazarian, A. 2005, *Theoretical and Computational Fluid Dynamics*, 19, 127
 Lazarian, A. 2004, *Journal of Korean Astronomical Society*, 37, 563
 Lazarian, A., & Pogosyan, D. 2000, *ApJ*, 537, 720
 Lazarian, A., & Pogosyan, D. 2004, *ApJ*, 616, 943
 Lazarian, A., & Pogosyan, D. 2006, *ApJ*, 652, 1348
 Lazarian, A., & Pogosyan, D. 2008, *ApJ*, 686, 350
 Pogosyan, D., & Lazarian, A. 2005, *Magnetic Fields in the Universe: From Laboratory and Stars to Primordial Structures.*, 784, 287
 Stanimirović, S., & Lazarian, A. 2001, *ApJ*, 551, L53

